

DEMONSTRATION FELs USING UC-XFEL TECHNOLOGIES AT THE SAMURAI LABORATORY

N. Majernik*, R. Robles†, G. Andonian, O. Camacho, A. Fukasawa,
G. Lawler, B. Naranjo, Y. Sakai, O. B. Williams, W. Lynn, J. B. Rosenzweig
UCLA, Los Angeles, CA, USA

Abstract

The ultra-compact x-ray free-electron laser (UC-XFEL), described in [1], combines several cutting edge beam physics techniques and technologies to realize an x-ray free electron laser at a fraction of the cost and footprint of existing XFEL installations. These elements include cryogenic, normally conducting RF structures for both the gun and linac, IFEL bunch compression, and short-period undulators. In this work, several stepping-stone, demonstrator scenarios under discussion for the UCLA SAMURAI Laboratory are detailed and simulated, employing different subsets of these elements. The cost, footprint, and technology risk for these scenarios are considered in addition to the anticipated engineering and physics experience gained.

INTRODUCTION

As described in [1], the ultra-compact x-ray free-electron laser (UC-XFEL) is a proposed approach to realizing a fifth generation light source, the next evolution of the modern x-ray free-electron laser. Although the concept can be applied to a range of photon energies and end-use cases, the most thoroughly developed version is a soft x-ray (SXR) UC-XFEL, delivering 25 gigawatts of 1.2 keV x-rays, which can fit in a 40 meter footprint for a total cost of \$40M, a fraction of existing, fourth generation XFELs, (~km and ~\$10⁹ respectively) while delivering performance which exceeds third generation (storage ring based) light sources by many orders of magnitude. The favorable scaling of the UC-XFEL will substantially increase access to intense, coherent, and ultra-fast XFEL beamtime, to the benefit of many scientific and industrial disciplines [2]. This model of affordable, distributed XFELs is often compared to the impact of ubiquitously available optical lasers on university and industry research for myriad fields.

Broadly speaking, the UC-XFEL hinges on several demonstrated but cutting-edge techniques and technologies to achieve these advancements. First among these is the use of advanced, short period, cryogenic undulators [3–7]. All extant XFELs rely on either pure permanent magnet (PPM) or hybrid Halbach arrays, at room temperature, with few centimeter periods. By using short period undulators, the UC-XFEL is able to reduce the required beam energy for a given x-ray wavelength, $\lambda_r = \frac{\lambda_u}{2\gamma^2} \left(1 + \frac{1}{2}K_u^2\right)$, where λ_u is the undulator period, γ is the beam Lorentz factor, and K_u is the undulator strength parameter. The (idealized)

exponential growth in radiated power along the undulator is characterized by the gain length, $L_g = \frac{\lambda_u}{4\pi\sqrt{3}\rho}$, [8] with the dimensionless Pierce parameter, $\rho = \left(\frac{I_e K_u^2 [JJ]^2}{16I_A \gamma^3 \sigma_x^2 k_z^2}\right)^{1/3}$, where [JJ] is a Bessel-function dependent parameter that is near unity for $K_u^2 < 1$, I_e is the beam current, I_A is the Alfvén current ≈ 17.045 kA, $k_u = 2\pi/\lambda_u$, and the transverse beam rms spot size is σ_x . All else held equal, the linac length scales with $\sqrt{\lambda_u}$ and the required undulator length, linearly proportional to L_g , scales with $\lambda_u^{5/6}$, which clearly motivates the desire to reduce the undulator period while not compromising on its strength.

However, a consequence of reducing the beam energy and undulator period is that more stringent requirements are set on the beam quality [9, 10]. By cryogenically cooling a C-band, normal-conducting copper photoinjector, higher launch fields can be supported, as well as reducing the thermal emittance, both of which contribute to the production of beams much brighter than those available from current FEL guns [11–13]. By using cryocooled copper linac segments, combined with an advanced rf distribution manifold design [14], the linac can provide accelerating gradients in excess of 125 MV/m, significantly higher than the gradients in existing XFELs, further reducing the UC-XFEL footprint.

Finally, it is vital to preserve the quality of these high brightness beams through their transport and, crucially, their compression to the high current levels required for efficient FEL operation. These beams are very susceptible to degradation by coherent synchrotron radiation (CSR) in conventional chicane compression so UC-XFEL relies on an advanced compression technique: inverse free-electron laser (IFEL) bunching [15]. In IFEL compression, the electron bunch is copropagated through a wiggler with a laser pulse, introducing periodic energy modulations, which can be transformed into a train of current spikes by a dispersive element. Such an approach suppresses collective effects which would degrade the beam quality in conventional compression.

DEMONSTRATOR FELs

Four of the technologies that enable the UC-XFEL are:

1. A cryogenic, high field photoinjector;
2. Cryogenic, manifold coupled linac segments;
3. IFEL compression;
4. A cryogenic, short period undulator.

* NMajernik@g.ucla.edu

† Now at Stanford University, Palo Alto, CA, USA

Table 1: Summary of Technology Overlap (Indicated with Bold Text), Parameters, and Simulated FEL Performance for the Visible FEL, EUV FEL, and SXR UC-XFEL

Parameter	Visible FEL	EUV FEL	SXR UC-XFEL
Photoinjector	Cryogenic C-band 1.6-cell	Existing S-band hybrid	Cryogenic C-band 1.6-cell
Acceleration	$1 \times \sim 1$ m cryogenic C-band linac section	$3 \times \sim 1$ m cryogenic C-band linac section	8×1 m cryogenic C-band linac section
Compression	Chicane or IFEL	Velocity bunching and long wavelength IFEL	CSR compensating chicane pair and IFEL
Undulator	Room temperature, conventional	Cryogenic, short period	Cryogenic, short period
Footprint	12 m	18 m	40 m
Budget	\$3M	\$12.5M	\$40M
Energy [MeV]	90	300	1000
Energy spread [%]	0.02	0.05	0.1
Total beam charge [pC]	100	100	100
Peak current [A]	200	1500	4000
Emittance [nm-rad]	60	400	70
Undulator period [mm]	20.6	6.5	6.5
Undulator field [T]	0.54	1	1
Undulator length [m]	2	4	4
Radiation wavelength [nm]	520	11	1
Radiation energy [eV]	2.4	110	1200
Gain length [m]	0.12	0.23	0.21
Peak power [MW]	160	170	25000

In this work, we detail two approaches for testing subsets of these elements given constraints on budget, footprint, and funder priorities. The first of these approaches is a visible FEL predicated on a \$3M grant emphasizing cryo-RF development while the second is an EUV FEL based on a \$12.5M grant with an emphasis on using proven systems. These two cases are discussed in detail below and summarized in Table 1 (with results based on GENESIS simulations [16]), highlighting the overlap between each case and the SXR UC-XFEL.

Visible FEL

For the \$3M visible FEL (see Fig. 1), based on funder preferences, the project is most appealing if considerable effort is put towards developing cryo-rf elements. This, combined with the relatively limited budget, results in a project that employs the same cryogenic C-band gun as would be used by the SXR UC-XFEL as well as the cryogenic C-band linac, albeit only one section for cost savings. However, the considerable expense of fabricating the short period undulator does not fit within this budget or prioritization so, instead, an existing, conventional undulator will be used. Specifically, the undulator from [17, 18], which was used in the first demonstration of a SASE FEL, is available for use at UCLA. This undulator, combined with the 90 MeV electron beam resulting from a single accelerating section, lases in the visible spectrum at 520 nm. Despite this mundane wavelength,

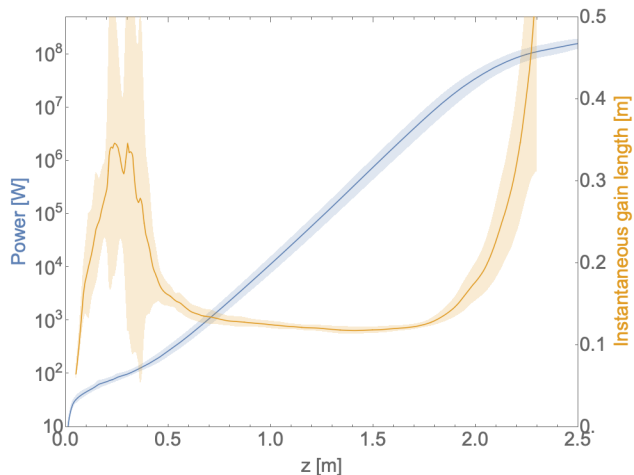


Figure 1: Plots showing the peak power (blue) and instantaneous gain length (orange) for GENESIS simulations of the visible FEL detailed in Table 1, but with the virtual undulator extending to 2.5 m to illustrate saturation. The shaded area corresponds to one standard deviation based on 16 SASE averaged runs.

the FEL will still serve as an extremely sensitive test of the coherent combination of all the other beamline components.

For the modest compression required by this application ($10\times$), both conventional compression and IFEL compression

sion are adequate. The beamline will be configured to allow both approaches to be used and contrasted. Resistive wall wakefields in the anomalous skin effect regime [19] must be considered for the full UC-XFEL but, due to the larger undulator gap and lower beam current, they will not be as impactful for this FEL. However, in addition to the FEL, we will directly characterize these effects using an adjustable, cryogenic, parallel plate setup.

As presently described, the visible FEL will not saturate, due largely to diffractive effects which arise from the long lasing wavelength [9, 10]. We are considering multiple options which will cause the FEL to saturate more rapidly including: higher compression factors, operating at different beam energies, or introducing waveguides into the undulator [20].

EUV FEL

For the \$12.5M EUV FEL (see Fig. 2), the design is directed by the program solicitation which encourages bold projects but does not support science or engineering research beyond the validation of operational readiness. With this guidance to reduce technology risk, the EUV FEL design relies exclusively on demonstrated technologies. In particular, although the principles of the high-gradient, cryogenic, C-band photoinjector have been explicated in detail [13], a functioning device has not been demonstrated. Therefore, an existing, state-of-the-art S-band hybrid photoinjector [21] serves as the electron source in this FEL design.

An additional constraint on this FEL design is the available space in the SAMURAI lab: the total beamline cannot exceed a length of 18 m. This led to the choice to use three, one meter cryogenic C-band linac sections, yielding a final energy of 300 MeV. This has the added benefit of serving as a “string test” to explore how devices which have been tested in isolation work together. The undulator for this FEL is a 4 meter, 6.5 mm period, cryogenically cooled undulator, like that demonstrated by [6]. An industrial partner has confirmed their willingness to produce this undulator for a price that fits within the project’s budget. An added benefit of this approach is that this undulator is the same as that required by the SXR UC-XFEL, providing a clear trajectory for future upgrades. With the 300 MeV beam, this FEL will lase in the EUV at 11 nm. This wavelength, long relative to the SXR’s 1 nm, leads to some additional challenges for this laser arising from slippage. Due to the highly constrained footprint, there is not space for substantial conventional compression, so the design relies on velocity bunching in the hybrid gun paired with IFEL compression. To mitigate the effects of slippage, the design employs a longer IFEL bunching wavelength: 40 μm vs SXR UC-XFEL’s 10 μm .

DISCUSSION

The UC-XFEL is an extremely promising concept, expected to deliver x-ray free-electron laser performance at a fraction of the price and footprint of existing XFELs. Although it is based on principles which are well established, it requires the careful integration of these subsystems. There-

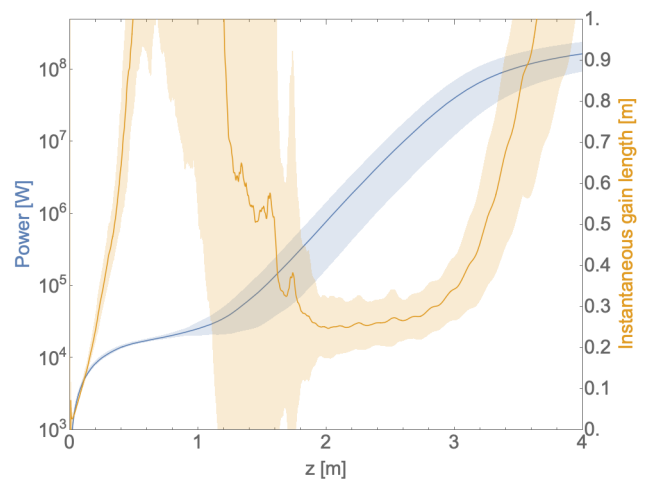


Figure 2: Plots showing the peak power (blue) and instantaneous gain length (orange) for GENESIS simulations of the EUV FEL detailed in Table 1. The shaded area corresponds to one standard deviation based on 16 SASE averaged runs. The large variation in shot-to-shot power is due to the high degree of slippage causing it to operate near single-spike mode.

fore, a staged approach to implementation may be valuable. To that end, this work presents two specific pathways this incremental approach may take. The first option is a visible FEL based on a \$3M grant and focuses heavily on the development of cryogenic rf components, notably including the construction of the photoinjector which would be used for the full UC-XFEL. The second option is an EUV FEL based on a \$12.5M grant which limits technology risk and instead focuses on integrating the demonstrated elements of the UC-XFEL. In particular, this would involve partnering with industry to produce the full, cryogenic, short-period undulator which would be required for the full UC-XFEL while relying on an existing S-band photoinjector as the electron source. Both cases would contribute substantially to the practical implementation of the UC-XFEL and would also acquire equipment that would be directly used in the final system.

ACKNOWLEDGMENTS

This work was supported by Department of Energy Grant DE-SC0020409 and National Science Foundation Grant No. PHY-1549132.

REFERENCES

- [1] J. B. Rosenzweig *et al.*, “An ultra-compact x-ray free-electron laser”, *New J. Phys.*, vol. 22, no. 9, p. 093067, 2020. doi: 10.1088/1367-2630/abb16c
- [2] C. Bostedt *et al.*, “Linac Coherent Light Source: The first five years”, *Rev. Mod. Phys.*, vol. 88, no. 1, p. 15007, Mar. 2016. doi:10.1103/RevModPhys.88.015007

- [3] N. Majernik and J. B. Rosenzweig, “Design of Comb Fabricated Halbach Undulators”, *Instruments*, vol. 3, p. 58, 2019. doi:10.3390/instruments3040058
- [4] F. H. O’Shea *et al.*, “Short period, high field cryogenic undulator for extreme performance x-ray free electron lasers”, *Phys. Rev. Spec. Top. Accel Beams*, vol. 13, no. 7, pp. 1–12, 2010. doi:10.1103/physrevstab.13.070702
- [5] A. Murokh *et al.*, “Textured dysprosium and gadolinium poles for high-field, short-period hybrid undulators”, *Nucl. Instrum. Methods Phys. Res., Sect. A*, vol. 735, pp. 521–527, 2014. doi:10.1016/j.nima.2013.10.020
- [6] F. H. O’Shea, R. Agustsson, Y.-C. Chen, A. J. Palmowski, and E. Spranza, “Development of a short period cryogenic undulator at RadiaBeam”, in *Proc. NAPAC’16*, Chicago, IL, USA, Oct. 2016, pp. 995-997. doi:10.18429/JACoW-NAPAC2016-WEPOB47
- [7] T. Tanaka and A. Kagamihata, “Demonstration of high-performance pole pieces made of monocrystalline dysprosium for short-period undulators”, *J. Synchrotron Radiat.*, vol. 26, pp. 1220–1225, 2019. doi:10.1107/s1600577519006052
- [8] R. Bonifacio, C. Pellegrini, and L. M. Narducci, “Collective instabilities and high-gain regime in a free electron laser”, *Opt. Commun.*, vol. 50, no. 6, pp. 373–378, Jul. 1984. doi:10.1016/0030-4018(84)90105-6
- [9] M. Xie, “Design optimization for an X-ray free electron laser driven by SLAC linac”, in *Proc. Particle Accelerator Conference (PAC’95)*, Dallas, TX, USA, May 1995, paper TPG10.
- [10] M. Xie, “Exact and variational solutions of 3D eigenmodes in high gain FELs”, *Nucl. Instrum. Methods Phys. Res., Sect. A*, vol. 445, no. 1, pp. 59–66, 2000. doi:10.1016/s0168-9002(00)00114-5
- [11] J. B. Rosenzweig *et al.*, “Ultra-high brightness electron beams from very-high field cryogenic radiofrequency photocathode sources”, *Nucl. Instrum. Methods Phys. Res., Sect. A*, vol. 909, pp. 224–228, 2018. doi:10.1016/j.nima.2018.01.061
- [12] J. B. Rosenzweig *et al.*, “Next generation high brightness electron beams from ultra high field cryogenic rf photocathode sources”, *Phys. Rev. Accel. Beams*, vol. 22, no. 2, p. 23403, 2019. doi:10.1103/physrevaccelbeams.22.023403
- [13] R. R. Robles *et al.*, “Versatile, high brightness, cryogenic photoinjector electron source”, *Phys. Rev. Accel. Beams*, vol. 24, no. 6, p. 063401, 2021. doi:10.1103/physrevaccelbeams.24.063401
- [14] S. Tantawi *et al.*, “Distributed coupling accelerator structures: A new paradigm for high gradient linacs”, *Phys. Rev. Accel. Beams*, vol. 23, p. 092001, 2020. doi:10.1103/PhysRevAccelBeams.23.092001
- [15] A. A. Zholents, “Method of an enhanced self-amplified spontaneous emission for x-ray free electron lasers”, *Phys. Rev. ST Accel. Beams*, vol. 8, p. 040701, Apr. 2005. doi:10.1103/physrevstab.8.040701
- [16] S. Reiche, “GENESIS 1.3: A fully 3D time-dependent FEL simulation code”, *Nucl. Instrum. Methods Phys. Res., Sect. A*, vol. 429, no. 1, pp. 243–248, 1999. doi:10.1016/s0168-9002(99)00114-x
- [17] M. J. Hogan *et al.*, “Measurements of gain larger than 10^5 at $12 \mu\text{m}$ in a self-amplified spontaneous-emission free-electron laser”, *Phys. Rev. Lett.*, vol. 81, no. 22, p. 4867, 1998. doi:10.1103/physrevlett.81.4867
- [18] N. Osmanov *et al.*, “UCLA-KIAE focusing permanent magnet undulator for SASE experiment”, *Nucl. Instrum. Methods Phys. Res., Sect. A*, vol. 407, no. 1, pp. 423–427, 1998. doi:10.1016/b978-0-444-82978-8.50087-7
- [19] G. Stupakov, K. Bane, P. Emma, and B. Podobodov, “Resistive wall wakefields of short bunches at cryogenic temperatures”, *Phys. Rev. ST Accel. Beams*, vol. 18, no. 3, pp. 1–6, 2015. doi:10.1103/physrevstab.18.034402
- [20] S. Reiche, J. Rosenzweig, and S. Telfer, “Proposal for a IR waveguide SASE FEL at the PEGASUS injector”, in *Proc. 19th Particle Accelerator Conf. (PAC’01)*, Chicago, IL, USA, Jun. 2001, paper WPPH120, pp. 2754–2756.
- [21] A. Fukasawa *et al.*, “Progress on the hybrid gun project at UCLA”, *Physics Procedia*, vol. 52, pp. 2–6, 2014. doi:10.1016/j.phpro.2014.06.002